PREDICTION AND MEASUREMENT OF THE VIBRATION AND ACOUSTIC RADIATION OF PANELS SUBJECTED TO ACOUSTIC LOADING

Travis L. Turner and Stephen A. Rizzi

Structural Acoustics Branch
NASA Langley Research Center
Hampton, VA 23681–0001 U.S.A.

INTRODUCTION

Interior noise and sonic fatigue are important issues in the development and design of advanced subsonic and supersonic aircraft. Conventional aircraft typically employ passive treatments, such as constrained layer damping and acoustic absorption materials, to reduce the structural response and resulting acoustic levels in the aircraft interior. These techniques require significant addition of mass and only attenuate relatively high frequency noise transmitted through the fuselage. Although structural acoustic coupling is in general very important in the study of aircraft fuselage interior noise, analysis of noise transmission through a panel supported in an infinite rigid baffle (separating two semi–infinite acoustic domains) can be useful in evaluating the effects of active/adaptive materials, complex loading, etc. Recent work has been aimed at developing adaptive and/or active methods of controlling the structural acoustic response of panels to reduce the transmitted noise[1]. A finite element formulation was recently developed to study the dynamic response of shape memory alloy (SMA) hybrid composite panels (conventional composite panel with embedded SMA fibers) subject to combined acoustic and thermal loads[2]. Further analysis has been performed to predict the far-field acoustic radiation using the finite element dynamic panel response prediction[3]. The purpose of the present work is to validate the panel vibration and acoustic radiation prediction methods with baseline experimental results obtained from an isotropic panel, without the effect of SMA.

EXPERIMENTAL SETUP AND PROCEDURE

The experiments were performed in the Transmission Loss Apparatus at NASA Langley Research Center, shown schematically in figure 1. The apparatus consists of a source room and a receiving room separated by a massive partition. A flat clamped aluminum panel ($0.3048 \times 0.1778 \times 1.1016 \times 10^{-3}$ m) was installed in a baffle mounted in the partition. Normal incidence acoustic excitation was provided by a speaker positioned approximately 0.9144 m from the panel. The source acoustic pressure was measured in the plane of the panel using one 1.27×10^{-2} m microphone with the panel removed from the baffle. The transmitted acoustic pressure was measured using a single vertical microphone array consisting of three 1.27×10^{-2} m microphones; one at the height of the panel center, one 0.3048 m above the center mic, and one 0.3048 m below the center mic. The panel vibration response was measured with a scanning laser vibrometer.

The speaker was driven by a random signal, band-pass filtered to a frequency range of 100–500 Hz. A centered 0.254×0.1016 m grid of 11 by 6 locations (total of 66 locations) was defined on the panel surface for vibration response measurements. Power spectra of the panel normal velocity at

these locations were acquired with the laser vibrometer and a spectrum analyzer. Magnitude and phase scans of the rms panel normal velocity over a finer 37 by 22 point grid were also performed to identify the modes corresponding to the first four panel natural frequencies. A 0.4×10^{-3} kg accelerometer attached to the panel served as a phase reference for the magnitude and phase scans. Transmitted acoustic pressure autospectra were collected at 21 locations by positioning the three–microphone array in each of seven measurement locations, defined in table 1 and shown schematically in figure 1. With the panel and clamping fixture removed from the baffle, incident pressure measurements were recorded in the plane of the panel, under identical source conditions to that of the response and transmitted pressure measurements. These source measurements were collected to assess the uniformity of the incident pressure across the panel and to provide input for the computational procedure. The overall sound pressure level in the plane of the panel at the opening center was approximately 109 dB (ref 20μPa).

Mic Position	Radial Distance (m)	Angle (deg)	Mic Position	Radial Distance (m)	Angle (deg)
R1	0.6096	0	R5	0.6096	-30
R2	1.2192	0	R6	1.2192	-30
R3	0.6096	30	R7	0.9144	-45
R4	1.2192	30			

Table 1: Receiving microphone array measurement locations, see figure 1.

COMPUTATIONAL METHOD

The panel vibration response and acoustic radiation predictions presented in this paper were generated using a previously developed computational method. The panel was modeled using a finite element analysis[2] and the radiated acoustic field was predicted using Rayleigh's integral[3]. The approach can easily include effects such as SMA fiber reinforcement, static large deflection thermal post-buckling, non-symmetric SMA distribution or lamination, and obliquely incident acoustic excitation of arbitrary temporal nature.

A 12x7 element mesh of 24 degree of freedom rectangular elements was used to model the structure. Torsional boundary springs were employed to match the measured fundamental frequency. The acoustic pressure loading on the panel can be considered to consist of the *blocked* pressure and the *radiated* pressure[4]. The blocked pressure is that pressure on the incident side when the panel is considered rigid and the radiated pressure is that due to panel motion. The acoustic radiation problem can be solved separately from the forced response of the panel by assuming that the radiated pressure is negligible compared to the blocked pressure. Thus, a source pressure spectrum obtained in the plane of the panel at the center of the baffle hole, when the panel and fixture were removed, was doubled and used as the blocked pressure input to determine the predicted panel response and acoustic radiation.

RESULTS AND DISCUSSION

The predicted results presented in this paper were generated using the following material properties for aluminum: E=68.9 Gpa, ν=0.33, and ρ=2751.4 kg/m^3. A torsional spring constant of 623 N was used in the finite element model to match the fundamental through fourth natural frequency.

The power spectral density of the pressure incident upon the panel is shown in figure 2. Comparisons of the predicted and measured panel normal velocity are shown in figure 3 for two measurement locations. The measurement location coordinates indicated in the figure are relative to the panel lower left corner. The agreement is excellent with the exception of the appearance of additional peaks in the measured spectra. These peaks are attributable to the first and second non-symmetric modes of the panel. The acoustic excitation generated by the speaker, although fairly uniform in magnitude, apparently was sufficiently oblique to excite the non-symmetric modes. It was assumed in the analysis that the incident pressure was uniform and normal. Thus, the non-symmetric modes do not appear in the predictions.

Typical results of a magnitude and phase scan are shown in figure 4 for a frequency interval around the third natural frequency. The magnitude and phase information are indicated by the contours and surface, respectively. The binary phase distribution (0 and $-\pi$) is indicative of a real vibration mode. Thus, the assumption in the predictions of a proportionally damped system is valid. Phase drop-out near the panel edges is an artifact of the very low velocities in these regions.

Comparisons of the predicted and measured transmitted pressure are shown in figure 5 for two measurement locations. It can be seen that the agreement is very good, particularly near the panel fundamental frequency. Theoretically, the pressure at the top and bottom microphones of the array should be the same, due to symmetry. However, the measured spectra showed an increase in the levels between the peaks with decreasing distance to the hard room floor. Thus, some of the discrepancies are attributable to receiving room reflections. Also note that the non-symmetric modes do not radiate, as expected.

CONCLUSIONS

Baseline experimental measurements of the response and acoustic radiation of an aluminum panel due to normally incident random acoustic excitation have been acquired. Computational predictions of the responses were made using a measured spectrum of the incident pressure as input. The prediction method is based upon a finite element model of the panel and Rayleigh's integral for the radiated acoustic field. Comparisons of the predicted and measured power spectral densities of the panel normal velocity and transmitted acoustic pressure show very good agreement, thus validating the prediction method. Minor discrepancies appear primarily attributable to uncertainties about the spatial characteristics of the incident pressure and acoustic reflections in the receiving room.

REFERENCES

1. Fuller, C. R.; Rogers, C. A.; and Robertshaw, H. H.: "Control of Sound Radiation with Active/Adaptive Structures," *Journal of Sound and Vibration*(1992) **157**(1), 19–39.

2. Turner, T. L.; Zhong, Z. W.; and Mei, C.: "Finite Element Analysis of the Random Response Suppression of Composite Panels at Elevated Temperatures Using Shape Memory Alloy Fibers," AIAA Paper No. 94–1324–CP, *Proceedings of the 35th Structures, Structural Dynamics, and Materials Conference*, Hilton Head, SC, April 18–21, 1994, pp. 136–146.

3. Turner, T. L.; Singh, M. P.; and Mei, C.: "A Spectral Analysis Approach for Acoustic Radiation from Composite Panels," AIAA Paper No. 95–1303–CP, *Proceedings of the 36th Structures, Structural Dynamics, and Materials Conference*, New Orleans, LA, April 10–13, 1995.

4. Roussos, L. A.: "Noise Transmission Loss of a Rectangular Plate in an Infinite Baffle," NASA TP-2398, March, 1985.

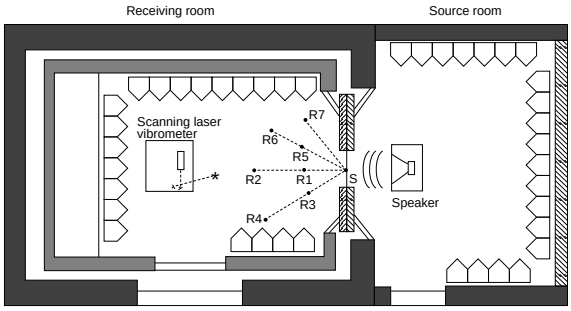

Figure 1: Schematic of the Transmission Loss Apparatus.

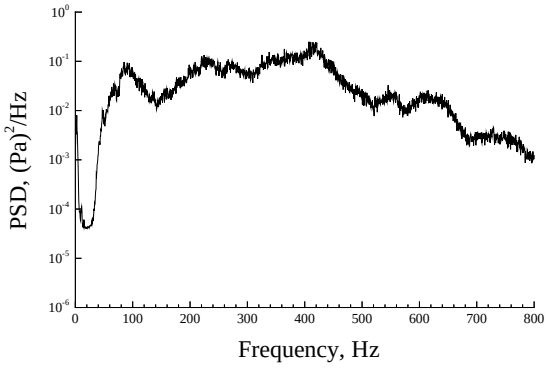

Figure 2: PSD of the acoustic excitation incident upon the panel (OASPL 109 dB).

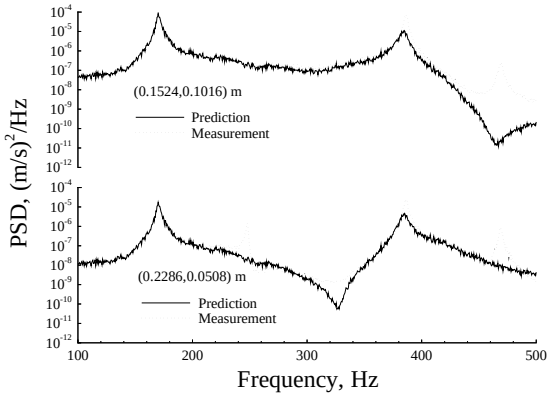

Figure 3: Comparison of predicted and measured panel normal velocity PSD at two locations (coordinates indicated in figure are relative to panel lower left corner).

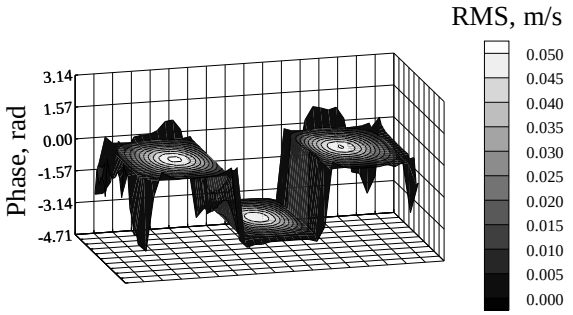

Figure 4: Superimposed magnitude and phase for the scan around the third natural frequency (386 Hz).

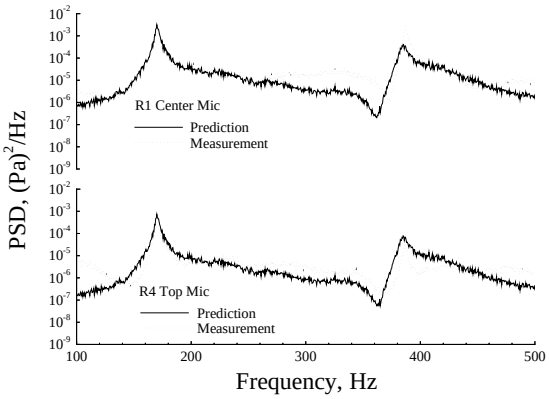

Figure 5: Comparison of the predicted and measured transmitted pressure PSD at two locations (defined in table 1 and figure 1).